NUMERICAL STUDY FOR MIXED CONVECTION FLOW OF OLDROYD-B NANOFLUID SUBJECT TO ACTIVATION ENERGY AND BINARY CHEMICAL REACTION

by

Dina ABUZAID and Malik Zaka ULLAH*

Department of Mathematics, Faculty of Science, King Abdulaziz University, Jeddah, Saudi Arabia

Original scientific paper
https://doi.org/10.2298/TSCI200214174A

This attempt discusses mixed convection Oldroyd-B nanoliquid-flow over a doubly stratified surface in existence of activation energy. Impacts of Brownian diffusion and thermophoretic are additionally accounted. The non-linear frameworks are simplified by suitable variables. Shooting method is utilized to develop a numeric solution of resulting issue. Graphs have been composed just to explore that how concentration and the temperature are impacted by different developing flow factors. Mass and heat transport rates are additionally tabulated and dissected. Furthermore, the temperature and concentration distributions are enhanced for larger thermophoresis parameter.

Key words: *Arrhenius activation energy. mixed convection flow, nanoparticles, double stratification, Oldroyd-B fluid, binary chemical reaction*

Introduction

The nanoparticle of size under 100 nm deferred into a standard fluid is named as nanoliquid. The essentialness of nanofluid is expected to their distinctive thermophysical qualities. Nanofluids show enormous capacity to lead power and heat, so it has a critical impact in industry. Nanoliquids have gotten extraordinary enthusiasm for its wide applications, for example, electronic chip cooling, hybrid powered machines, progressed atomic frameworks, laser-helped sedate conveyance, solar liquid heating, microchips, excessively proficient magnets and opto-electronics and so on. Just because, Choi [1] exhibited the term nanoparticle inundated into a common fluid. Buongiorno [2] presented a numerical model for warm transport in nanoliquid, including the impacts of Brownian scattering and thermophoretic dispersion. Further applicable examinations on nanofluids are -cited by the investigations [3-18].

Species of concentration contrast exist in a blend subject to mass transport wonder. By fluctuating centralization of species in blend move those from high focus locale to low fixation area. Least mandatory vitality that is needed by reactants before occuring substance reaction is termed as activation energy. Mass move mechanism with concoction reaction with activation energy by and the large discovers practicals in mechanics of oil and water emulsions, synthetic building, nourishment preparing, *etc.* Right off bat common convection flow of paired blend in porous space subject to initiation vitality is proposed by Bestman [19]. Makinde *et al.* [20] numerically examined insecure normal convective stream with enactment vitality and nth-request response. Maleque *et al*. [21] discussed endothermic/exothermic response in mixed convective

* Corresponding author, e-mail: zmalek@kau.edu.sa

streams with initiation vitality. Changed Arrhenius work has been utilized by Awad *et al.* [22] so as to consider flimsy pivoting stream of parallel liquid past a rash twisted surface. Casson liquid stream subject to initiation vitality is tended to by Abbas *et al.* [23]. Shafique *et al.* [24] inspected numerically the pivoting viscoelastic stream fusing artificially receptive species with actuation vitality. Anuradha and Yegammai [25] talked about paired concoction response and initiation vitality in radiative hydromagnetic nanoliquid-flow by vertical surface. Khan *et al.* [26] analyzed impacts of enactment vitality and entropy in radiative nanomaterial flow. Further ongoing endeavors on activation energy are -cited by attempts [27-30].

Inspired by aforementioned attempts, the motivation here is to explore importance of binary chemical response and activation energy in mixed convection Oldroyd-B nanoliquid-flow with solutal and thermal stratifications. Random movement and thermophoretic phenomenas occur in the existence of nanofluid. Resulting scientific framework is understood numerically via shooting technique. Concentration, temperature, Sherwood and Nusselt factors are also analyzed.

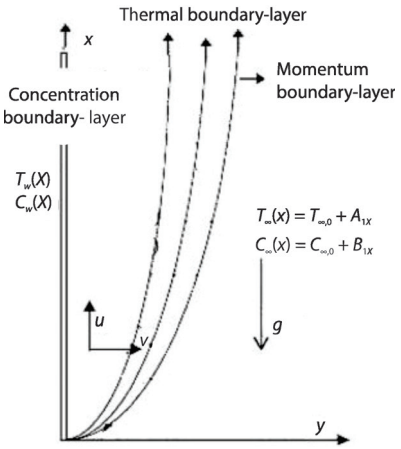

Figure 1. Flow model and co-ordinate system

Problem development

We examine 2-D doubly stratified mixed convection Oldroyd-B nanoliquid-flow with binary chemical response and activation energy. Flow is induced by extending sheet at $y = 0$. Flow occupies the region $y > 0$, fig. 1. Brownian dispersion and thermophoretic impacts are likewise present. The governing expressions of Oldroyd-B nanoliquid-flow [28, 31]:

$$\frac{\partial u}{\partial x}+\frac{\partial v}{\partial y}=0 \tag{1}$$

$$u\frac{\partial u}{\partial x}+v\frac{\partial u}{\partial y}+\lambda_1\left(u^2\frac{\partial^2 u}{\partial x^2}+v^2\frac{\partial^2 u}{\partial y^2}+2uv\frac{\partial^2 u}{\partial x\partial y}\right)=\nu\frac{\partial^2 u}{\partial y^2}+$$
$$+\nu\lambda_2\left(u^2\frac{\partial^3 u}{\partial x\partial y^2}+v^2\frac{\partial^3 u}{\partial y^3}-\frac{\partial u}{\partial x}\frac{\partial^2 u}{\partial y^2}-\frac{\partial u}{\partial y}\frac{\partial^2 v}{\partial y^2}\right)+\mathrm{g}\left[\beta_T\left(T-T_\infty\right)+\beta_C\left(C-C_\infty\right)\right] \tag{2}$$

$$u\frac{\partial T}{\partial x}+v\frac{\partial T}{\partial y}=\alpha\frac{\partial^2 T}{\partial y^2}+\frac{(\rho c)_p}{(\rho c)_f}\left[D_B\left(\frac{\partial T}{\partial y}\frac{\partial C}{\partial y}\right)+\frac{D_T}{T_\infty}\left(\frac{\partial T}{\partial y}\right)^2\right] \tag{3}$$

$$u\frac{\partial C}{\partial x}+v\frac{\partial C}{\partial y}=D_B\frac{\partial^2 C}{\partial y^2}+\frac{D_T}{T_\infty}\left(\frac{\partial^2 T}{\partial y^2}\right)-k_r^2\left(C-C_\infty\right)\left(\frac{T}{T_\infty}\right)^n\exp\left(-\frac{E_a}{\kappa T}\right) \tag{4}$$

Subjected boundary conditions [31]:

$$u=U_w\left(x\right),\ v=0,\ T=T_w\left(x\right),\ C=C_w\left(x\right)\ \text{at}\ \ y=0 \tag{5}$$

$$u\to 0,\ T\to T_\infty\left(x\right)=T_{\infty,0}+A_1x,\ C\to C_\infty\left(x\right)=C_{\infty,0}+B_1\ \text{as}\ \ y\to\infty \tag{6}$$

where u and v are the stand for velocities in x- and y-axes, n – the for fitted rate constant, E_a – the activation energy, μ – the dynamic viscosity, $(\rho c)_f$ – the heat capacity of fluid, D_B – the Brownian factor, κ – the Boltzmann constant, T – the temperature, λ_1 – the relaxation time,

$\nu = \mu/\rho$ – the kinematic viscosity, β_C – the concentration expansion factor, $(\rho c)_p$ – the effective heat capacity of nanoparticles, k_r – the reaction rate, k – the thermal conductivity, λ_2 – the retardation time, g – the gravitational acceleration, D_T – the thermophoretic factor, β_T – the thermal expansion factor, ρ – the density, C – the concentration, $\alpha = k/(\rho c)_f$ – the thermal diffusivity, T_∞ and T_w – the ambient and surface temperatures, and C_∞ and C_w – the ambient and surface concentrations. Thus:

$$U_w(x) = cx,\ T_w(x) = T_{\infty,0} + M_1 x,\ C_w(x) = C_{\infty,0} + N_1 x \tag{7}$$

where c, A_1, B_1, M_1, N_1, $T_{\infty,0}$, and $C_{\infty,0}$ stand for positive constants. Non-dimensional variables are defined:

$$\begin{gathered} u = cxf'(\eta),\ v = -\sqrt{c\nu}\,f(\eta),\ \eta = \sqrt{\frac{c}{\nu}}y,\ \theta(\eta) = \frac{T - T_{\infty,0}}{\Delta T} - \frac{A_1 x}{\Delta T},\ \Delta T = T_w(x) - T_{\infty,0} = M_1 x \\ \phi(\eta) = \frac{C - C_{\infty,0}}{\Delta C} - \frac{B_1 x}{\Delta C},\ \Delta C = C_w(x) - C_{\infty,0} = N_1 x \end{gathered} \tag{8}$$

Equation (1) is now identically verified and eqs. (2)-(7) yield:

$$f''' + ff'' - f'^2 + \beta_1\left(2ff'f'' - f^2 f'''\right) + \beta_2\left(f''^2 - ff^{iv}\right) + \lambda(\theta + N\phi) = 0 \tag{9}$$

$$\theta'' + \mathrm{Pr}\left(f\theta' - f'\theta - \varepsilon_1 f' + Nb\theta'\varphi' + Nt\theta'^2\right) = 0 \tag{10}$$

$$\phi'' + \mathrm{Sc}\left(f\phi' - f'\phi - \varepsilon_2 f'\right) + \frac{Nt}{Nb}\theta'' - \sigma\mathrm{Sc}(1+\delta\theta)^n \phi\exp\left(-\frac{E}{1+\delta\theta}\right) = 0 \tag{11}$$

$$f = 0,\ f' = 1,\ \theta = 1 - \varepsilon_1,\ \phi = 1 - \varepsilon_2 \ \text{ at } \ \eta = 0 \tag{12}$$

$$f' \to 0,\ f'' \to 0,\ \theta \to 0,\ \phi \to 0 \ \text{ as } \ \eta \to \infty \tag{13}$$

where Nb stands for Brownian motion parameter, β_2 and β_1 – the Deborah numbers in terms of retardation and relaxation times, ε_2 – the solutal stratification, Re_x – the local Reynolds number, δ – the temperature difference parameter, λ – the mixed convection number, Nt – the thermophoresis number, Gr_x – the Grashof parameter, E – the non-dimensional activation energy, σ – the chemical reaction parameter, N – the buoyancy ratio, Pr – the Prandtl number, ε_1 – the thermal stratification, and Sc – the Schmidt number. These parameters are expressed:

$$\begin{gathered} \beta_1 = \lambda_1 c,\ \beta_2 = \lambda_2 c,\ \lambda = \frac{\mathrm{Gr}}{\mathrm{Re}_x^2},\ \mathrm{Gr}_x = \frac{g\beta_T \Delta T x^3}{\nu^2},\ \delta = \frac{T_w - T_\infty}{T_\infty},\ \mathrm{Re}_x = \frac{U_w x}{\nu} \\ N = \frac{\beta_C \Delta C}{\beta_T \Delta T},\ \mathrm{Pr} = \frac{\nu}{\alpha},\ Nb = \frac{(\rho c)_p}{(\rho c)_f}\frac{D_B \Delta C}{\nu},\ Nt = \frac{(\rho c)_p}{(\rho c)_f}\frac{D_T \Delta T}{\nu T_\infty}, E = \frac{E_a}{\kappa T_\infty} \\ \varepsilon_1 = \frac{x}{\Delta T}\frac{\mathrm{d}}{\mathrm{d}x}\left[T_\infty(x)\right],\ \mathrm{Sc} = \frac{\nu}{D_B},\ \varepsilon_2 = \frac{x}{\Delta C}\frac{\mathrm{d}}{\mathrm{d}x}\left[C_\infty(x)\right],\ \sigma = \frac{k_r^2}{c} \end{gathered} \tag{14}$$

Local Nusselt, Nu_x, and the Sherwood, Sh_x, factors:

$$\mathrm{Nu}_x = -\frac{x}{(T_w - T_\infty)}\left.\frac{\partial T}{\partial y}\right|_{y=0} = -(\mathrm{Re}_x)^{1/2}\theta'(0) \tag{15}$$

$$\mathrm{Sh}_x = -\frac{x}{\left(C_w - C_\infty\right)}\frac{\partial C}{\partial y}\bigg|_{y=0} = -\left(\mathrm{Re}_x\right)^{1/2}\phi'(0) \tag{16}$$

Graphical results and discussion

The arrangements of administering framework are figured by utilizing shooting strategy. This segment presents impacts of various pertinent parameters including Deborah numbers β_2 and β_1, mixed convection parameter, λ, thermophoresis parameter, Nt, activation energy, E, Brownian movement parameter, Nb, warm stratification parameter, ε_1, concoction response parameter, σ, and solutal stratification, ε_2, on temperature, $\theta(\eta)$, and concentration, $\phi(\eta)$. Variation in temperature, $\theta(\eta)$, for varying Deborah number, β_1, is appeared in fig. 2. Here temperature profile is more for bigger Deborah number, β_1. Impact of Deborah number, β_1, on temperature, $\theta(\eta)$, is shown in fig. 3. It is plainly indicated that temperature, $\theta(\eta)$, is diminishing capacity of Deborah number, β_2. A correlation of figs. 2 and 3 shows that β_1 and β_2 have very inverse consequences for temperature field. Physically β_1 includes unwinding time while β_2 comprises of hindrance time. Bigger unwinding time prompts higher temperature while bigger hindrance time compares to a lower temperature. In this way an improvement in β_1 produces more temperature while bigger β_2 portrays less temperature. Figure 4 presents bigger estimations of blended convection parameter, λ, comparing to bring down temperature, $\theta(\eta)$. Figure 5 presents impact of warm stratification, ε_1, on temperature, $\theta(\eta)$. Temperature $\theta(\eta)$ is diminishing capacity of the warm stratification parameter ε_1. Physically nearness of warm stratification impact diminishes viable temperature contrast among surface and encompassing liquid which prompts a flimsier temperature. It is additionally seen that instance of recommended surface temperature is recouped when $\varepsilon_1 = 0$. Thermophoresis and Brownian movement impacts on temperature, $\theta(\eta)$ are exhibited in figs. 6 and 7 individually. Temperature profile is higher for bigger estimations of thermophoresis and Brownian movement. Physically nearness of nanoparticles builds warm

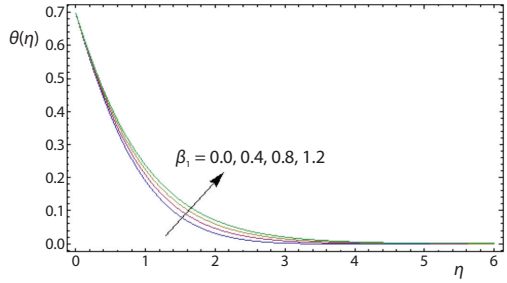

Figure 2. Curves of $\theta(\eta)$ for β_1

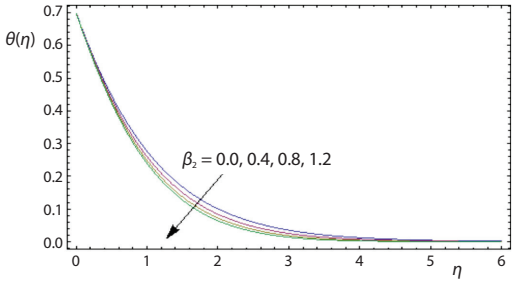

Figure 3. Curves of $\theta(\eta)$ for β_2

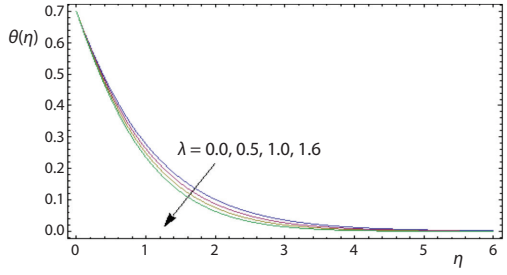

Figure 4. Curves of $\theta(\eta)$ for λ

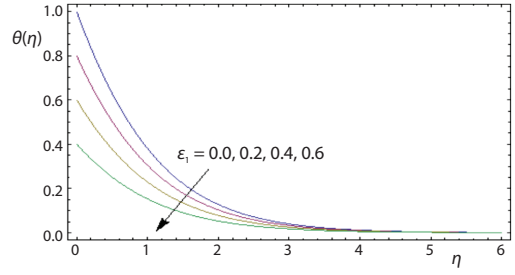

Figure 5. Curves of $\theta(\eta)$ for ε_1

conductivity of liquid. An expansion in thermophoresis and Brownian movement compares to high warm conductivity. Such high warm conductivity makes upgrade in the temperature field. Figure 8 shows variety in concentration, $\phi(\eta)$, for different estimations of Deborah number, β_1. Here concentration is improved with expansion in the Deborah number, β_1. Figure 9 displays that bigger Deborah number, β_2, produces a decrease in concentration, $\phi(\eta)$. Figure 10 shows change in concentration, $\phi(\eta)$, comparing to various estimations of blended convection parameter, λ. Clearly concentration, $\phi(\eta)$, is lower for bigger estimations of blended convection parameter, λ. Impact of solutal stratification, ε_2, on concentration, $\phi(\eta)$, is plotted in fig. 11. It is unmistakably noted that concentration, $\phi(\eta)$, is reduced when solutal stratification, ε_2, enlarges. For $\varepsilon_2 = 0$, recommended surface concentration circumstance is accomplished. Impact of thermophoresis parameter, Nt, on concentration, $\phi(\eta)$, is shown in fig. 12. Concentration, $\phi(\eta)$, is expanding capacity of thermophoresis parameter, Nt. Figure 13 shows that concentration, $\phi(\eta)$, is lower for bigger estimations of Brownian movement parameter, Nb. Figure 14 delineates that bigger estimations of compound response parameter, σ, prompts lower concentration. Figure 15 clarifies effect of E on concentration, $\phi(\eta)$. An improvement in E prompts higher concentration, $\phi(\eta)$. Table 1 presents numerical estimations of heat move rate $-\theta'(0)$ for particular estimations of blended convection parameter, λ. It is seen that heat move rate is higher when expanding es-

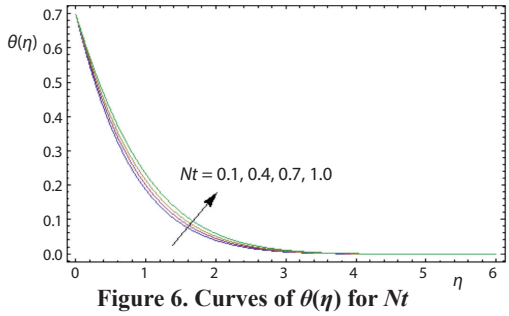

Figure 6. Curves of $\theta(\eta)$ for Nt

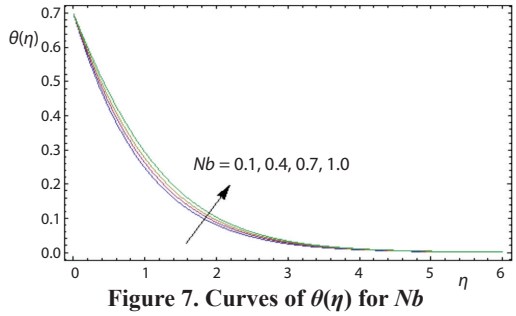

Figure 7. Curves of $\theta(\eta)$ for Nb

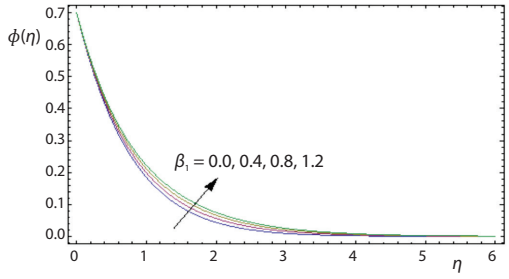

Figure 8. Curves of $\phi(\eta)$ for β_1

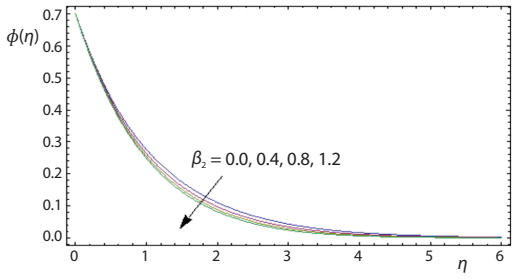

Figure 9. Curves of $\phi(\eta)$ for β_2

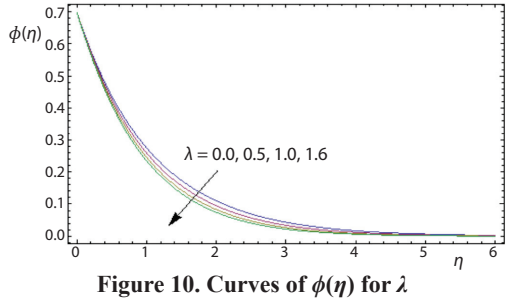

Figure 10. Curves of $\phi(\eta)$ for λ

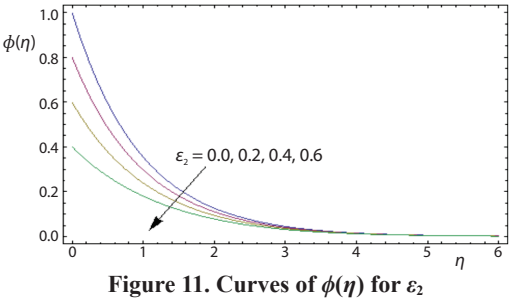

Figure 11. Curves of $\phi(\eta)$ for ε_2

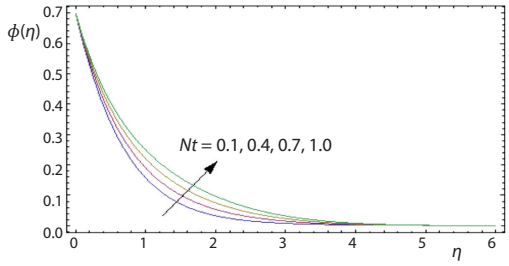

Figure 12. Curves of $\phi(\eta)$ for Nt

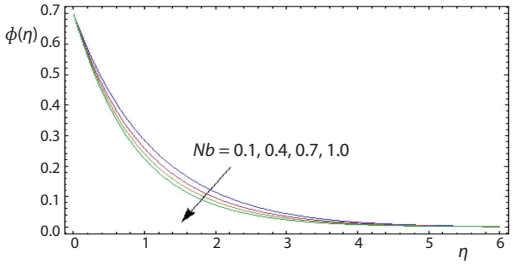

Figure 13. Curves of $\phi(\eta)$ for Nb

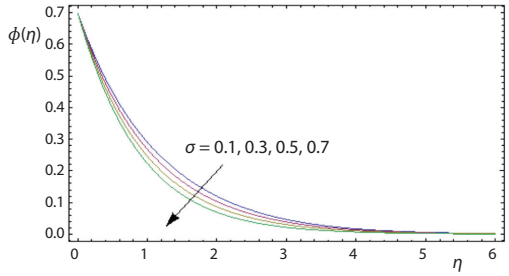

Figure 14. Curves of $\phi(\eta)$ for σ

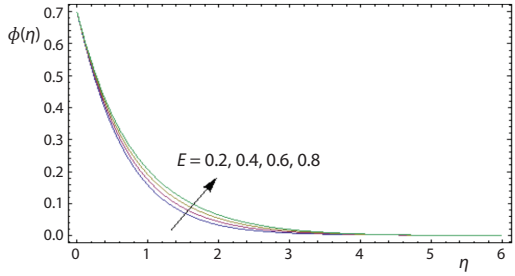

Figure 15. Curves of $\phi(\eta)$ for E

timations of blended convection parameter, λ, are accounted. Table 2 delineates mass move rate $-\phi'(0)$ for particular values of blended convection parameter, λ. Here we saw that mass move rate has higher estimations for bigger blended convection parameter, λ.

Table 1. Heat transfer rate $-\theta(0)$ for varying λ when $\beta_1 = \beta_2 = 0.2$, $N = 0.1$, $\delta = 0.3$, $E = 0.5$, $Nt = 0.2$, Pr = Sc = 1.0, Nb = 0,5, and $\varepsilon_1 = \varepsilon_2 = 0.3$

λ	0.0	0.2	0.4	0.6
$-\theta'(0)$	0.66692	0.67715	0.68496	0.62975

Table 2. Mass transfer rate $-\phi'(0)$ for varying λ when $\beta_1 = \beta_2 = 0.2$, $N = 0.1$, $\delta = 0.3$, $E = 0.5$, $Nt = 0.2$, Pr = Sc = 1.0, Nb = 0,5, and $\varepsilon_1 = \varepsilon_2 = 0.3$

λ	0.0	0.2	0.4	0.6
$-\phi'(0)$	0.66692	0.67715	0.68496	0.69205

Conclusions

Importance of double stratification in mixed convection Oldroyd-B nanoliquid-flow with binary chemical response and activation energy is inspected. Both temperature and concentration are enhanced when we increment β_1. Both temperature and concentration have been reduced for larger estimations of mixed convective number. Impacts of solutal and thermal stratification numbers on concentration and temperature, respectively are similar. The present results reduces to Newtonian fluid-flow situation when $\beta_1 = \beta_2 = 0$.

Acknowledgment

This project was funded by the Deanship of Scientific Research (DSR) at King Abdulaziz University, Jeddah, under grant No. G: 1458-247-1440. The authors, therefore, acknowledge with thanks DSR for technical and financial support.

References

[1] Choi, S. U. S., Estman, J. A., Enhancing Thermal Conductivity of Fluids with Nanoparticles, *Proceedings,* ASME International Mechanical Engineering Congress and Exposition, San Francisco, Cal., USA, 1995
[2] Buongiorno, J., Convective Transport in Nanofluids, *Journal Heat Transfer*, *128* (2006), 3, pp. 240-250

[3] Eastman, J. A., *et al*., Anomalously Increased Effective Thermal Conductivities of Ethylene Glycol-Based Nanofluids Containing Copper Nanoparticles, *Appl. Phys. Lett*., *78* (2001), 6, pp. 718-720
[4] Tiwari, R. K., Das, M. K., Heat Transfer Augmentation in a Two-Sided Lid-Driven Differentially Heated Square Cavity Utilizing Nanofluid, *Int. J. Heat Mass Transf.*, *50* (2007), 9-10, pp. 2002-2018
[5] Abu-Nada, E., Oztop, H. F., Effects of Inclination Angle on Natural-Convection in Enclosures Filled with Cu-Water Nanofluid, *Int. J. Heat Fluid-Flow*, *30* (2009), 4, pp. 669-678
[6] Khan, J. A., *et al*., On Model for 3-D Flow of Nanofluid: An Application Solar Energy, *Journal Mol. Liq*., *194* (2014), June, pp. 41-47
[7] Mansur, S., Ishak, A., The 3-D Flow and Heat Transfer of a Nanofluid Past a Permeable Stretching Sheet with a Convective Boundary Condition, *AIP Conference Proceedings*, *1614* (2014), 1, pp. 906-912
[8] Hayat, T., *et al*., Magnetohydrodynamic 3-D Flow of Viscoelastic Nanofluid in the Presence of Non-Linear Thermal Radiation, *Journal Magn. Magn. Mater*., *385* (2015), July, pp. 222-229
[9] Muhammad, T., *et al*., A Revised Model for Darcy-Forchheimer Flow of Maxwell Nanofluid Subject to Convective Boundary Condition, *Chinese J. Phys*., *55* (2017), 3, pp. 963-976
[10] Hayat, T., *et al*., An Analytical Solution for Magnetohydrodynamic Oldroyd-B Nanofluid-Flow Induced by a Stretching Sheet with Heat Generation/Absorption, *Int. J. Thermal Sci*., *111* (2017), Jan., pp. 274-288
[11] Muhammad, T., *et al*., A Revised Model for Darcy-Forchheimer 3-D Flow of Nanofluid Subject to Convective Boundary Condition, *Results Phys*., *7* (2017), pp. 2791-2797
[12] Hayat, T. *et al*., On Magnetohydrodynamic Flow of Nanofluid Due to a Rotating Disk with Slip Effect: A Numerical Study, *Comp. Methods Appl. Mech. Eng*., *315* (2017), Mar., pp. 467-477
[13] Hussain, Z., *et al*., The 3-D Convective Flow of CNT Nanofluids with Heat Generation/Absorption Effect: A Numerical Study, *Comp. Methods Appl. Mech. Eng*., *329* (2018), Feb., pp. 40-54
[14] Selimefendigil, F., Oztop, H. F., Mixed Convection of Nanofluids in a 3-D Cavity with Two Adiabatic Inner Rotating Cylinders, *Int. J. Heat Mass Transfer*, *117* (2018), Feb., pp. 331-343
[15] Muhammad, T., *et al*., Significance of Darcy-Forchheimer Porous Medium in Nanofluid through Carbon Nanotubes, *Commun. Theoret. Phys*., *70* (2018), 3, p. 361
[16] Hayat, T., *et al*., On Model for 3-D Flow of Nanofluid with Heat and Mass Flux Boundary Conditions, *Journal Thermal Sci. Eng. Appl*., *10* (2018), 3, 031003
[17] Mahanthesh, B., *et al*., The MHD Flow of SWCNT and MWCNT Nanoliquids Past a Rotating Stretchable Disk with Thermal and Exponential Space Dependent Heat Source, *Physica Scripta*, *94* (2019), 8, 085214
[18] Saif, R. S., *et al*., Darcy-Forchheimer Flow of Nanofluid Due to a Curved Stretching Surface, *Int. J. Numer. Methods Heat Fluid-Flow*, *29* (2019), 1, pp. 2-20
[19] Bestman, A. R., Natural-Convection Boundary-Layer with Suction and Mass Transfer in a Porous Medium, *Int. J. Energy Res*., *14* (1990), 4, pp. 389-396
[20] Makinde, O. D., *et al*., Unsteady Convection with Chemical Reaction and Radiative Heat Transfer Past a Flat Porous Plate Moving through a Binary Mixture, *Africka Matematika*, *22* (2011), Feb., pp. 65-78
[21] Maleque, K. A., *et al*., Effects of Exothermic/Endothermic Chemical Reactions with Arrhenius Activation Energy on MHD Free Convection and Mass Transfer Flow in Presence of Thermal Radiation, *Journal Thermodyn*., *2013* (2013), 692516
[22] Awad, F. G., *et al*., Heat and Mass Transfer in Unsteady Rotating Fluid-Flow with Binary Chemical Reaction and Activation Energy, *Plos One*, *9* (2014), 9, e107622
[23] Abbas, Z., *et al*., Numerical Solution of Binary Chemical Reaction on Stagnation Point Flow of Casson Fluid over a Stretching/Shrinking Sheet with Thermal Radiation, *Energy*, *95* (2016), Jan., pp. 12-20
[24] Shafique, Z., *et al*., Boundary-Layer Flow of Maxwell Fluid in Rotating Frame with Binary Chemical Reaction and Activation Energy, *Results Phys*., *6* (2016), pp. 627-633
[25] Anuradha, S., Yegammai, M., The MHD Radiative Boundary-Layer Flow of Nanofluid Past a Vertical Plate with Effects of Binary Chemical Reaction and Activation Energy, *Glob. J. Pure Appl. Math*., *13* (2017), 9, pp. 6377-6392
[26] Khan, M. I., *et al*., Entropy Generation Minimization and Binary Chemical Reaction with Arrhenius Activation Energy in MHD Radiative Flow of Nanomaterial, *Journal Mol. Liq*., *259* (2018), June, pp. 274-283
[27] Hayat, T., Numerical Simulation for Darcy-Forchheimer 3-D Rotating Flow Subject to Binary Chemical Reaction and Arrhenius Activation Energy, *Journal Central South Uni*., *26* (2019), June, pp. 1250-1259
[28] Hayat, T., *et al*., Effects of Binary Chemical Reaction and Arrhenius Activation Energy in Darcy-Forchheimer 3-D Flow of Nanofluid Subject to Rotating Frame, *Journal Thermal Anal. Calorimet*., *136* (2019) Oct., pp. 1769-1779

[29] Asma, M., *et al*., Numerical Study for Darcy-Forchheimer Flow of Nanofluid Due to a Rotating Disk with Binary Chemical Reaction and Arrhenius Activation Energy, *Mathematics*, *7* (2019), 10, 921
[30] Asma, M., Numerical Study for Magnetohydrodynamic Flow of Nanofluid Due to a Rotating Disk with Binary Chemical Reaction and Arrhenius Activation Energy, *Symmetry*, *11* (2019), 10, 1282
[31] Hayat, T., Temperature and Concentration Stratification Effects in Mixed Convection Flow of an Oldroyd-B Fluid with Thermal Radiation and Chemical Reaction, *PloS One*, *10* (2015), 6, e0127646

Paper submitted: February 14, 2020
Paper revised: April 5, 2020
Paper accepted: April 9, 2020

© 2021 Society of Thermal Engineers of Serbia
Published by the Vinča Institute of Nuclear Sciences, Belgrade, Serbia.
This is an open access article distributed under the CC BY-NC-ND 4.0 terms and conditions